also shows, by comparing columns 3 and 4, that only two optimizations with $p = 2$ of the ξ algorithm yield, for engineering purposes, essentially equal-ripple responses. For a 50-dB specification the final solution has characteristic impedances[1] of 0.606 595, 0.303 547, 0.722 287, 0.235 183, 0.722 287, 0.303 547, and 0.606 595 with deviations from specifications of $-0.028\,245$ (equal to at least 5 figures).

CONCLUSIONS

Two new algorithms and related results for the least pth approach to minimax design have been presented. Documented computer programs are available from J. W. Bandler at a nominal charge. A more detailed presentation of this material is also available [11].

REFERENCES

[1] J. W. Bandler and C. Charalambous, "Practical least pth optimization of networks," *IEEE Trans. Microwave Theory Tech. (1972 Symp. Issue)*, vol. MTT-20, pp. 834–840, Dec. 1972.

[2] ——, "New algorithms for network optimization," *IEEE Trans. Microwave Theory Tech. (1973 Symp. Issue)*, vol. MTT-21, pp. 815–818, Dec. 1973.

[3] ——, "Nonlinear minimax optimization as a sequence of least pth optimization with finite values of p," *Int. J. Syst. Sci.*, to be published.

[4] J. W. Bandler, C. Charalambous, and J. H. K. Chen, "MINOPT—An optimization program based on recent minimax results," Faculty Eng., McMaster Univ., Hamilton, Ont., Canada, Rep. SOC-70, Dec. 1974.

[5] J. W. Bandler and W. Y. Chu, "FLOPT2—A program for least pth optimization with extrapolation to minimax solutions," Faculty Eng., McMaster Univ. Hamilton, Ont., Canada, Rep. SOC-84, Apr. 1975.

[6] C. Charalambous, "Minimax optimization of recursive digital filters using recent minimax results," *IEEE Trans. Acoust., Speech, Signal Processing*, vol. ASSP-23, pp. 333–345, Aug. 1975.

[7] A. V. Fiacco and G. P. McCormick, *Nonlinear Programming: Sequential Unconstrained Minimization Techniques*. New York: Wiley, 1968.

[8] W. Y. Chu, "Extrapolation in least pth approximation and nonlinear programming," Faculty Eng., McMaster Univ., Hamilton, Ont., Canada, Rep. SOC-71, Dec. 1974.

[9] R. Fletcher, "FORTRAN subroutines for minimization by quasi-Newton methods," Atomic Energy Research Establishment, Harwell, Berks., England, Rep. AERE-R7125, 1972.

[10] M. C. Horton and R. J. Wenzel, "General theory and design of optimum quarter-wave TEM filters", *IEEE Trans. Microwave Theory Tech.*, vol. MTT-13, pp. 316–327, May 1965.

[11] J. W. Bandler, C. Charalambous, J. H. K. Chen, and W. Y. Chu, "New results in the least pth approach to minimax design," Faculty Eng., McMaster Univ., Hamilton, Ont., Canada, Rep. SOC-80, Mar. 1975.

[1] Actually symmetrical to at least the accuracy of the CDC 6400.

Analysis of the Transient Temperature Distribution in a Stripline with Triple-Layer Dielectric

MASAKI SASAKI, NORINOBU YOSHIDA,
ICHIRO FUKAI, MEMBER, IEEE, AND JUN-ICHI FUKUOKA

***Abstract*—The transient temperature distributions in the cross section of a stripline with triple-layer dielectric substrate are found by employing the finite element method. The calculations for three cases of different depths of center conductor considered as heat source are shown.**

For each case, the calculated temperature distributions are shown at $t = 10$ s when the temperature variation has a large gradient in time and at the steady state.

Manuscript received September 10. 1975; revised September 10, 1975.

The authors are with the Faculty of Engineering, Hokkaido University, Sapporo, Japan.

With the integralization of electric devices and the appearance of high-power semiconductor devices, miniaturization of transmission systems has become necessary. In dealing with such systems, it is of considerable importance to confirm the rise and distribution of temperatures appearing in the operation of the devices in as much as they are in a risk of thermal destruction and thermal degeneration. For the analysis of these problems, some theoretical methods and numerical procedures have been proposed. There are, however, various difficulties in the analysis of such theoretical methods.

In the present analysis, the finite element method based on the variational method was used because of its advantage in dealing with the complicated contours as well as composite media. In relation to the heat conduction equation in a two-dimensional case, the functional is defined as [1]

$$\chi = \iint \left\{ \tfrac{1}{2}k \left[\left(\frac{\partial T}{\partial x}\right)^2 + \left(\frac{\partial T}{\partial y}\right)^2 \right] - \left(q - C\frac{\partial T}{\partial t}\right) T \right\} dx\, dy \qquad (1)$$

where T is the temperature, C the heat capacity, k heat conductivity, and q the rate of heat generation. The temperature rise and distribution can be obtained by finding the function T by which the functional χ is made stationary. To carry out the preceding method, the domain is divided into many triangular elements, χ is differentiated with respect to T, the derivative is set equal to zero. The resulting equation is thus given by

$$\left\{\frac{\partial x}{\partial T_n}\right\} = \sum \left\{\frac{\partial x}{\partial T_n}\right\}^e = [H]\{T\} + [P]\left\{\frac{\partial T}{\partial t}\right\} - \{K\} = 0 \qquad (2)$$

where $[H]$ is the heat conductivity matrix, $[P]$ is the heat capacity matrix, and $\{K\}$ is a vector which expresses the distribution of heat sources. Applying the trapezoidal approximation for the derivative with respect to time, the following difference equation was obtained for all nodal temperatures in a matrix form

$$\left([H] + \frac{2}{\Delta t}[P]\right)\{T\}_t = [P]\left(\left\{\frac{\partial T}{\partial t}\right\}_{t-\Delta t} + \frac{2}{\Delta t}\{T\}_{t-\Delta t}\right) + \{K\}_t. \qquad (3)$$

To illustrate the correctness of the method, we employed a simple problem where heat source q $(=100\ \mathrm{W/cm^3})$ distributes uniformly in the square column of alumina with infinite length under the Newton cooling condition. The temperature rise at the center of the column obtained by both the exact analytical solution and by the finite element method are shown in Fig. 1, and difference between the two methods is within one percent.

Then the temperature characteristics are calculated for striplines with triple-layer dielectric media. The analytical model is shown in Fig. 2 where $H = W_2 = 0.1$ cm, $a_1 = a_2 = a_3 = H/3$, $W_1 = 10a_1$, and $b = 0.001$ cm. For symmetry, the right half-plane is considered. The center medium is alumina, the heat source material is copper, and other media are glass. The respective thermal constants are shown in Table I. The rate of heat generation per unit volume q is $10^4\ \mathrm{W/cm^3}$. The boundary condition at the surface where $x = 0$ is

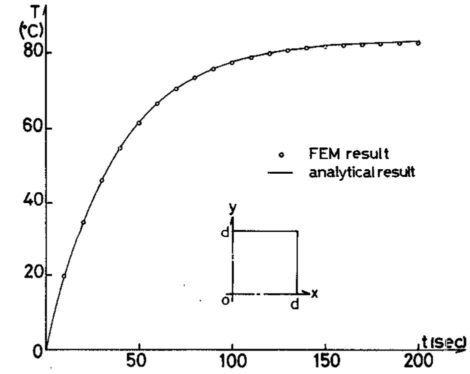

Fig. 1. Example 1: Geometry of the problem and the temperature rise at center of heat source. $d = 0.5$ mm.

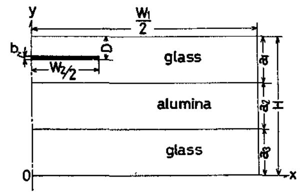

Fig. 2. Example 2: Geometry of the problem. $H = W_2 = 0.1$ cm, $a_1 = a_2 = a_3 = H/3$, $W_1 = 10a_1$, $b = 0.001$ cm, and $D = 0, a_1/2, a_1$.

TABLE I
THERMAL CONSTANTS

Material	Heat conductivity w/cm°C	Heat capacity J/cm^3°C	Heat transfer coefficient w/cm^2°C
Copper	4.1	3.77	
Glass	0.014	1.73	0.003
Alumina	0.251	4.45	

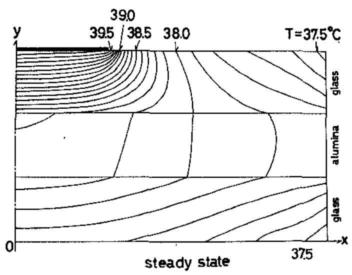

Fig. 3. The equitemperature lines in a steady state with $D = 0$.

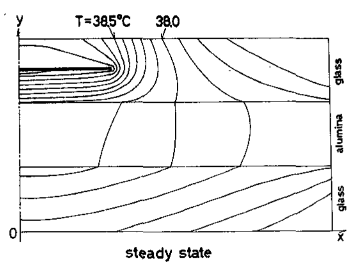

Fig. 4. The equitemperature lines in a steady state with $D = a_1/2$.

nonconductive, i.e., the normal gradient of temperature is zero, and at the other surface, convection loss is equal to $\alpha(T - T_a)$ where α is the heat transfer coefficient and T_a is the ambient temperature. The calculation is achieved for three values of parameter D depth of heat source. These values are $D = 0, a_1/2, a_1$. As for the components of $[P]$ and $\{K\}$ in (3), for better convergence of this numerical calculation, lumped coefficients [2] are adopted instead of the consistent coefficients used by Flatabø [1].

The calculated results are shown in Figs. 3–9. Figs. 3–5 show equitemperature lines in the cross section of striplines for each value of parameter D in a steady state. Figs. 6–8 show the same at $t = 10$ s. Fig. 9 shows the temperature rise at each center of heat sources for $t = 0$–10 s.

In these three cases, temperatures at the center of the heat source in a steady state are lower than 40°C. In these three cases, when comparing the steady state with that at $t = 10$ s, in the lower glass layers, the equitemperature lines in the former have a

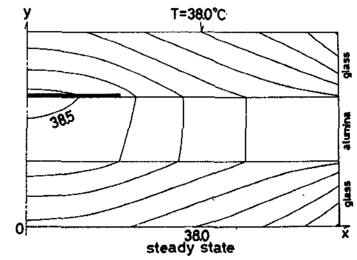

Fig. 5. The equitemperature lines in a steady state with $D = a_1$.

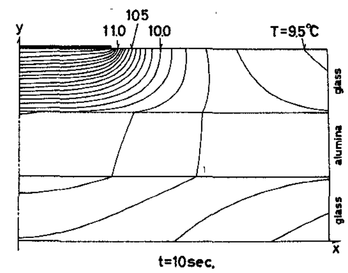

Fig. 6. The equitemperature lines at $t = 10$ s with $D = 0$.

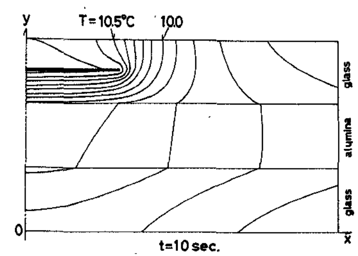

Fig. 7. The equitemperature lines at $t = 10$ s with $D = a_1/2$.

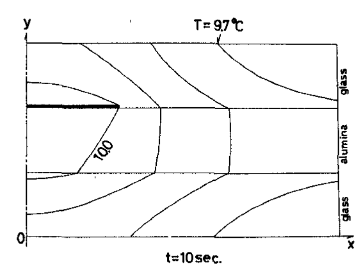

Fig. 8. The equitemperature lines at $t = 10$ s with $D = a_1$.

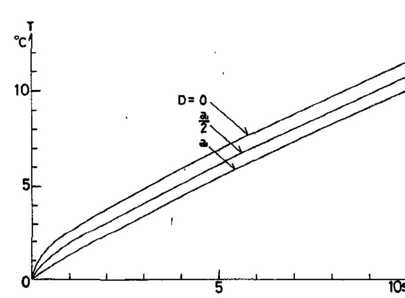

Fig. 9. The temperature rises at center of heat sources.

gentler gradient to the x axis than the latter. At the substrate edges, the temperatures in alumina layers are higher than in the glass layers. In the alumina layers, equitemperature lines are almost vertical to the x axis. In the case of $D = a_1/2$, the temperature gradient above the heat source is gentler than under it. These phenomena are regarded as due to the thermal energy generated at heat sources being diffused through alumina layers of high conductivity and then radiated out of the substrate.

The temperature rise at center of the heat source where the temperature characteristics are remarkably affected by parameter D is gentler at $D = a_1$ than others, and similarly the maximum temperature is lower than in others, because of the direct contact with alumina of a high conductivity. Thus it may be said that the case of $D = a_1$ has less thermal risk than others.

To ensure the correctness of this method for numerical analysis, the case of single-layer dielectric media which has infinite width of substrate is calculated by the finite element method with equivalent heat transfer coefficient at the finite boundary and by the analytical method. And both results agree very well. The band matrix method which is well known as one of the elimination procedures is employed so as to reduce the computing time.

For a detailed analysis, the dielectric loss in the substrate is considered as well as the joule loss in the center strip, but in the present analysis only the joule loss is considered for simplicity. The analysis containing the dielectric loss and the nonlinearity of the thermal characteristics of the media is achieved by the finite element method in the same manner as in the preceding cases without much difficulty. For nonlinear problems, it may be useful to apply the method for the plasticity problem in structural mechanics, e.g., the incremental initial strain method.

REFERENCES

[1] N. Flatabø, "Transient heat conduction in power cables solved by the finite element method," *IEEE Trans. Power App. Syst.*, vol. PAS-92, pp. 56–63, Jan./Feb. 1973.

[2] K. H. Huebner, *Finite Element Method for Engineers.* New York: Wiley, 1975.